

Small Scale Anisotropy Predictions for the Auger Observatory

Daniel De Marco[†], Pasquale Blasi[‡] and Angela V. Olinto[¶]

[†] Bartol Research Institute, University of Delaware Newark, DE 19716, U.S.A.

[‡] INAF/Osservatorio Astrofisico di Arcetri, Largo E. Fermi, 5 - 50125 Firenze, ITALY

[¶] Department of Astronomy & Astrophysics, Kavli Institute for Cosmological Physics, 5640 S. Ellis Ave. Chicago, IL 60637, U.S.A.

E-mail: ddm@bartol.udel.edu, blasi@arcetri.astro.it, olinto@oddjob.uchicago.edu

Abstract. We study the small scale anisotropy signal expected at the Pierre Auger Observatory in the next 1, 5, 10, and 15 years of operation, from sources of ultra-high energy (UHE) protons. We numerically propagate UHE protons over cosmological distances using an injection spectrum and normalization that fits current data up to $\sim 10^{20}$ eV. We characterize possible sources of ultra-high energy cosmic rays (UHECRs) by their mean density in the local Universe, $\bar{\rho} = 10^{-r} \text{ Mpc}^{-3}$, with r between 3 and 6.

These densities span a wide range of extragalactic sites for UHECR sources, from common to rare galaxies or even clusters of galaxies. We simulate 100 realizations for each model and calculate the two point correlation function for events with energies above 4×10^{19} eV and above 10^{20} eV, as specialized to the case of the Auger telescope. We find that for $r \gtrsim 4$, Auger should be able to detect small scale anisotropies in the near future. Distinguishing between different source densities based on cosmic ray data alone will be more challenging than detecting a departure from isotropy and is likely to require larger statistics of events. Combining the angular distribution studies with the spectral shape around the GZK feature will also help distinguish between different source scenarios.

1. Introduction

There are two main open questions that together constitute the long standing mystery of the origin of ultra-high energy cosmic rays (UHECRs): 1) What is their acceleration site? 2) Does their diffuse spectrum at the Earth possess the so-called GZK feature [1], evidence of their inelastic interaction with the photons of the cosmic microwave background (CMB)? In the next years the Pierre Auger Observatory [2] will provide us with important hints to the first question and will most likely answer the second question. Moreover, it can be expected that this experiment will open the way to realistic measurements of the chemical composition of cosmic rays at the highest energies, another important piece of the puzzle.

As the Southern site of the Auger Observatory nears completion, an increase by one order of magnitude of the worldwide exposure to the highest energy particles is within reach. The energy range between 10^{19} eV and 10^{20} eV is of particular importance as it provides a window for charged particle astronomy. Cosmic rays in this energy range suffer smaller deflections by cosmic magnetic fields than their lower energy counterparts, although at the lowest end of this range the effects of the galactic magnetic field are expected to be important. However one can imagine to be potentially able to correct for this effect or even use it to infer the topology of the magnetic field of the Galaxy.

A key element in determining the origin of UHECRs is the detection of large [3] and small scale anisotropies in their arrival directions. If, as expected and as suggested by some numerical simulations (see, e.g., [4]), the deflection of cosmic rays of energies larger than $\sim 4 \times 10^{19}$ eV should be small, then to some extent they should point back to their source. As large numbers of cosmic rays at such energies are observed, the pointing becomes more easily feasible. The net result is the appearance of small angle clustering in the arrival directions, and the strength of the effect is related to the mean density of sources in the universe.

In addition, interactions of cosmic rays with the cosmic background radiation limit the distance from which cosmic rays with energies above $\sim 10^{20}$ eV can reach the Earth to ~ 50 Mpc. The matter distribution within a 50 Mpc radius from the Earth is rather anisotropic, thus large scale anisotropies in the UHECR arrival direction distribution should also be observable.

An important piece of information, necessary to infer the origin of UHECRs is their dominant chemical composition as a function of energy. The present observational information about the composition at the highest energies is rather poor and does not allow us to draw any firm conclusions. While our calculations are carried out for a purely proton composition at the highest energies, an appreciable contamination of heavier nuclei may change our conclusions on the implications of small angle clustering to some extent. From the theoretical point of view, a proton-dominated or a mixed composition also have quite different implications on the transition of cosmic rays from a galactic to an extragalactic origin: while a mixed composition would imply that such transition takes place at the *ankle* [5, 6], a pure proton composition (or very light pollution from heavier nuclei) would imply that the transition occurs at lower energies (*dip* scenario) [7].

Our conclusions regarding small scale anisotropies should apply more generally with the caveat that we assume the best fit injection spectrum for a pure proton source, which is softer than the mixed composition case [6] (however, see [8] for the effect of magnetic fields in the source region and [9] for the effect of maximum energies

depending on the source). Given that the relevant energy range is limited (between 4×10^{19} eV and 10^{20} eV), small differences in the injection should not have a significant effect.

The unknown magnitude and structure of the magnetic fields outside the Milky Way limit our ability to predict the precise energy threshold for charged particle astronomy. The role of extragalactic magnetic fields in changing the spectrum and clustering of UHECRs is also badly constrained as different simulations give different estimates for the magnitude and spatial structure of these fields (see, e.g., [4, 10]). The combined effect of a mixed composition and significant extragalactic fields may move the threshold for detecting anisotropies to larger energies (see, e.g., [11]). Here, we assume that extragalactic magnetic fields can be neglected for particles with energies above 4×10^{19} eV. This assumption holds if magnetic fields in the extragalactic medium are less than ~ 0.1 nG with a reversal scale of ~ 1 Mpc and the small scale anisotropies are evaluated on angles of $\sim 1^\circ$ [12, 13]. This magnitude field is compatible with observational bounds [14] and detailed numerical simulations such as [4] (however, see [10] for different numerical estimates). UHECR observations will eventually allow us to measure the strength of the extragalactic magnetic field and get information about its structure (see, e.g., [15, 16]). In the mean time, searches for small scale anisotropies should focus on energy thresholds from 4×10^{19} eV to 10^{20} eV.

The mean density of UHECR sources can be determined once small scale anisotropies (SSAs) in the arrival directions are observed. Thus far the only experiment to report departures from isotropy is AGASA [17]. The statistical significance of the clustering has been challenged [18] as it depends on the angular scale chosen for binning the data. Assuming the AGASA data, the number density of sources was estimated to range from $\sim 10^{-6}$ Mpc $^{-3}$ to $\sim 10^{-4}$ Mpc $^{-3}$ with large uncertainties [12, 13, 19, 20]. In Refs. [12, 13], full numerical simulations of the propagation were performed which account for the statistical errors in the energy determination and the AGASA acceptance. The first study concluded that the AGASA small scale anisotropies indicated a density of sources $\sim 10^{-5}$ Mpc $^{-3}$ [12]. However, when taken together with the observed AGASA spectrum, the SSAs and the GZK feature become inconsistent [13].

Here we study the small scale anisotropy signal expected at the Pierre Auger Observatory in the next 1, 5, 10, and 15 years. We numerically propagate ultra high energy protons over cosmological distances and characterize possible sources by their mean density in the local Universe, $\bar{\rho} = 10^{-r}$ Mpc $^{-3}$, with r between 3 and 6. These source densities span the relevant range of extragalactic sites for UHECR sources, from galaxies to clusters of galaxies. In §2 we review our numerical approach and present the SSA results of 100 realizations of each model. We show the two point correlation functions for events of energies above 4×10^{19} eV and above 10^{20} eV, list the expected number of doublets, and discuss the expected spectrum for different models. In §3, we discuss the implications of our results and conclude.

2. Small Scale Anisotropies and Spectra at Auger

The propagation of UHECRs is simulated using the Monte-Carlo code described in [21]. We assume that UHECRs are protons injected with a power-law spectrum by extragalactic sources. The injection spectrum is taken to be of the form:

$$F(E) \propto E^{-\gamma} \exp(-E/E_{\max}), \quad (1)$$

where γ is the spectral index and E_{\max} is the maximum injection energy at the source. We fix $\gamma = 2.6$ and $E_{\max} = 10^{21.5}$ eV since these values reproduce well the experimental results in the lower energy high statistics region around $\sim 10^{18.5}$ eV up to $\sim 10^{20}$ eV (see, e.g. [21]). We focus on events above 4×10^{19} eV, which are generated at $z \ll 1$, therefore, source evolution is only marginally relevant [12]. We simulate the propagation of protons from the source to the observer by including the photo-pion production, pair production, and adiabatic energy losses due to the expansion of the Universe. We assume the Universe has matter and dark energy densities as fractions of the critical density given by $\Omega_m = 0.3$ and $\Omega_\Lambda = 0.7$, respectively.

Our source distribution in space is generated by a random placement of sources for a given spatial density and particles are emitted from randomly chosen source positions. The source redshifts are generated with a probability distribution proportional to

$$\frac{dn}{dz} \propto r(z)^2 \frac{dt}{dz}, \quad (2)$$

where dt/dz gives the relation between time and redshift (see, e.g., the expression given in [22]) and $r(z)$ is defined as

$$r = c \int_{t_g}^{t_0} \frac{dt}{R(t)}, \quad (3)$$

where t_g is the age of the Universe when the event was generated, t_0 is the present age of the Universe, and $R(t)$ is the scale factor of the Universe. Once a particle has been generated, the code propagates it to the detector calculating energy losses and taking into account the detector energy and angular resolution. The source angular coordinates on the celestial sphere are chosen randomly from a uniform distribution in right ascension and with a declination distribution proportional to $\cos \delta$.[‡] Since we neglect the effects of the magnetic fields on the propagation, we ignore sources outside the experimental field of view and assign to visible sources a probability proportional to:

$$r(z)^{-2} \omega(\delta), \quad (4)$$

where $r(z)^{-2}$ takes into account the distance dependence of the solid angle and $\omega(\delta)$ is the relative exposure of the experiment in the given direction.

For a given simulated set of events, we calculate the angular two point correlation function as defined in [19, 23] to study the expected departure from an isotropic distributions in the sky. For each event, the number of events within a circle at an angular distance θ and a bin width $\Delta\theta$ is summed:

$$N(\theta) = \frac{1}{S(\theta)} \sum_{i>j} R_{ij}(\theta), \quad (5)$$

and divided by the area $S(\theta) = 2\pi |\cos(\theta) - \cos(\theta + \Delta\theta)|$ of the angular bin between θ and $\theta + \Delta\theta$, and $R_{ij}(\theta) = 0, 1$ counts the events in the same bin.

For the Auger observatory in the Southern Hemisphere, we assume a total acceptance of $7,000 \text{ km}^2 \text{ sr}$ independent of energy above 10^{19} eV. For the angular resolution we used 1° , for the energy resolution 20%, and for the exposure dependence on the arrival direction we used the analytical estimate given in Ref. [3]. By

[‡] The declination δ is defined as being 0° on the equatorial plane and $\pm 90^\circ$ at the poles, so $d\Omega = \cos \delta d\delta d\alpha$.

Table 1. Number of events expected with $E > 10^{20}$ eV.

$\bar{\rho}$ (Mpc $^{-3}$)	$n_{20} / 1\text{yr}$ $n_{19.6} = 70$	$n_{20} / 5\text{yr}$ $n_{19.6} = 350$	$n_{20} / 10\text{yr}$ $n_{19.6} = 700$	$n_{20} / 15\text{yr}$ $n_{19.6} = 1050$
cont.	2.9 ± 1.7	14 ± 4	29 ± 5	43 ± 6
10^{-3}	2.5 ± 1.3	13 ± 3	26 ± 6	39 ± 8
10^{-4}	2.0 ± 1.4	10 ± 4	22 ± 6	34 ± 7
10^{-5}	1.6 ± 1.5	7.3 ± 3.3	14 ± 5	20 ± 7
10^{-6}	0.4 ± 0.7	2.1 ± 1.7	4.2 ± 2.9	7.2 ± 4.3

comparison, AGASA had an acceptance of 160 km 2 sr and reported 886 events above 10^{19} eV over a decade with an accumulated exposure of 1,645 km 2 sr yr. If the two experiments had the same energy calibration, Auger would accumulate over $\sim 10^4$ events above 10^{19} eV in 5 years of operation. However, the first released Auger spectrum [24] suggests that the energy calibration of AGASA [25] is systematically high and, consequently, a lower flux is observed for a fixed energy at Auger.

We normalize our simulations to the Auger flux above 4×10^{19} eV [24] (indicated in Table 1 as $n_{19.6}$: number of events above 4×10^{19} eV) and determine the number of events with energy above 10^{20} eV as a result of our simulations. These numbers are summarized in Table 1, for a continuous distribution of sources and for different values of the source density.

The numbers in Table 1 require some further comments: the spectrum of cosmic rays as detected by Auger at the present time is rather odd, in that it appears to have a dip instead of a bump at energies around 4×10^{19} eV. This may easily lead to an incorrect estimate of the number of events expected at higher energies. In Fig. 1 we show the Auger data and the predicted spectrum as normalized at low energies (10^{19} eV, dashed line) and at 4×10^{19} eV (solid line). Systematic uncertainties on the flux and on the energy determination are indicated by double arrows at two different energies [24].

The figure clearly illustrates the fact that the normalization at 4×10^{19} eV may cause an underestimate of the number of events expected at higher energies, since most likely the feature observed at that energy is the result of a statistical fluctuation. In order to keep memory of this problem we carry out our analyses for both instances of normalization.

The number of events as obtained with the higher normalization are reported in Table 2, and are systematically higher by a factor ~ 2 .

We parametrize the mean density for the distribution of sources by $\bar{\rho} = 10^{-r}$ Mpc $^{-3}$, and choose r between 3 and 6. The mean densities of extragalactic astrophysical accelerators of UHECRs should be well represented by this range which covers galaxies, groups and clusters of galaxies. For example, black holes in centers of normal galaxies should have $r \simeq 3$ while those in active galaxies should have

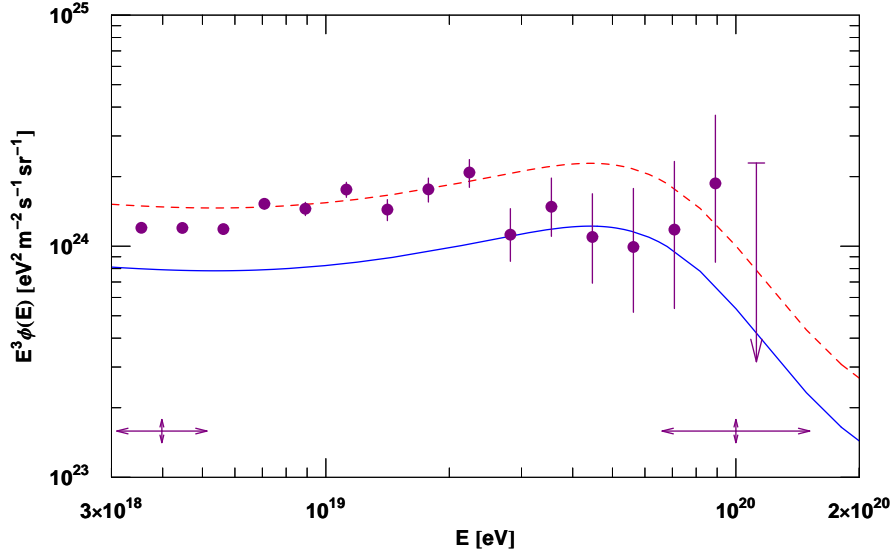


Figure 1. Data points from the Pierre Auger Observatory [24] compared with theoretical predictions normalized at different energies.

Table 2. Number of events expected with $E > 10^{20}$ eV using the normalization of the spectrum at low energy.

$\bar{\rho}$ (Mpc^{-3})	$n_{20} / 1\text{yr}$ $n_{19.6} = 120$	$n_{20} / 5\text{yr}$ $n_{19.6} = 600$	$n_{20} / 10\text{yr}$ $n_{19.6} = 1200$	$n_{20} / 15\text{yr}$ $n_{19.6} = 1800$
cont.	5.0 ± 2.2	25 ± 5	50 ± 7	75 ± 8
10^{-3}	4.2 ± 1.8	22 ± 5	44 ± 9	67 ± 11
10^{-4}	3.6 ± 2.0	18 ± 5	38 ± 9	58 ± 12
10^{-5}	2.5 ± 1.8	13 ± 5	24 ± 8	35 ± 10
10^{-6}	0.8 ± 1.0	3.5 ± 2.3	7.4 ± 4.2	13 ± 7

$r \gtrsim 6$. Similar densities are expected for rich clusters of galaxies. The most common extragalactic objects that may house UHECR sources are galaxies, which have $\bar{\rho}$ depending on their type and luminosity ranging from $r = 2$ to 3. For example, the Sloan Digital Sky survey recently reported a comprehensive study [26] of galaxy clustering in a large volume limited sample at relatively low redshifts (z between 0.015 and 0.1). In their samples, galaxy number densities vary between $2 \times 10^{-2} h^3 \text{Mpc}^{-3}$ (in their sample with limiting r -magnitude -18) to $6 \times 10^{-3} h^3 \text{Mpc}^{-3}$ (for the brighter sample). The number density in groups of galaxies range from $6 \times 10^{-4} h^3 \text{Mpc}^{-3}$ (starting with groups of 3 galaxies) to richer clusters with $10^{-7} h^3 \text{Mpc}^{-3}$. Choosing the Hubble parameter, $h = H_0/100 \text{ km/s/Mpc} = 0.75$, the observed $\bar{\rho}$ range

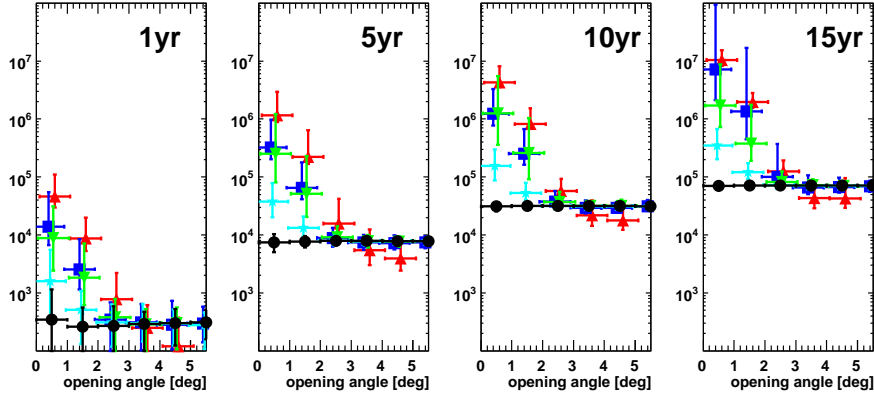


Figure 2. Two point correlation function expected for Auger events above 4×10^{19} eV after 1, 5, 10, and 15 years, for continuous distribution of sources (black circles), and number densities of 10^{-3} Mpc^{-3} (cyan stars), 10^{-4} Mpc^{-3} (green downward triangles), 10^{-5} Mpc^{-3} (blue squares), and 10^{-6} Mpc^{-3} (red upward triangles). No limitation on the minimum distance for sources were imposed. Error bars are asymmetric 1σ . The data points in this and in all subsequent figures have been slightly offset (horizontally) for clarity of presentation.

from 8×10^{-3} Mpc^{-3} to 4×10^{-8} Mpc^{-3} . As we discuss below, detecting SSAs for $\bar{\rho} \gtrsim 10^{-3}$ Mpc^{-3} will require many years of observations, while $\bar{\rho} \ll 10^{-6}$ Mpc^{-3} may generate higher UHECR clustering than reported so far, unless magnetic fields move the threshold for charged particle astronomy to energies around 10^{20} eV. Such low densities of sources however would generate a sharp GZK cutoff in the diffuse spectrum, starting at energies even below 10^{20} eV. This situation appears to be disfavored even on the basis of current data.

2.1. Two point correlation function above 4×10^{19} eV

Figure 2 shows the two point correlation function of simulated events with energies above 4×10^{19} eV for the full Auger South aperture and exposures after 1, 5, 10, and 15 years of operation. The number of events is normalized at the Auger data at energy 4×10^{19} eV. The black circles show a continuous distribution of sources, while sources with number densities of 10^{-3} Mpc^{-3} are represented by cyan stars, 10^{-4} Mpc^{-3} by green downward triangles, 10^{-5} Mpc^{-3} by blue squares, and 10^{-6} Mpc^{-3} by red upward triangles. The error bars are asymmetric 1σ standard deviations calculated in each energy bin for events above and below the mean. It is clear from this figure that after one year with the full Auger South aperture a discrete distribution with $\bar{\rho} \lesssim 10^{-4}$ Mpc^{-3} should be distinguishable from a continuous source distribution. After 5 years, even a $\bar{\rho} \sim 10^{-3}$ Mpc^{-3} can be detected at the few σ level. After a decade, departure from continuous should be detected at many tens of σ .

Although departures from continuous distributions should become clear soon, distinguishing between different specific source densities in Fig. 2 is more difficult.

In the 100 realizations for the assumptions in Fig. 2, there are often configurations with sources within 10 Mpc. These randomly placed nearby sources produce a significant dispersion in the two point correlation function at small opening angles and generate an overlap between different choices of $\bar{\rho}$. To help distinguish between

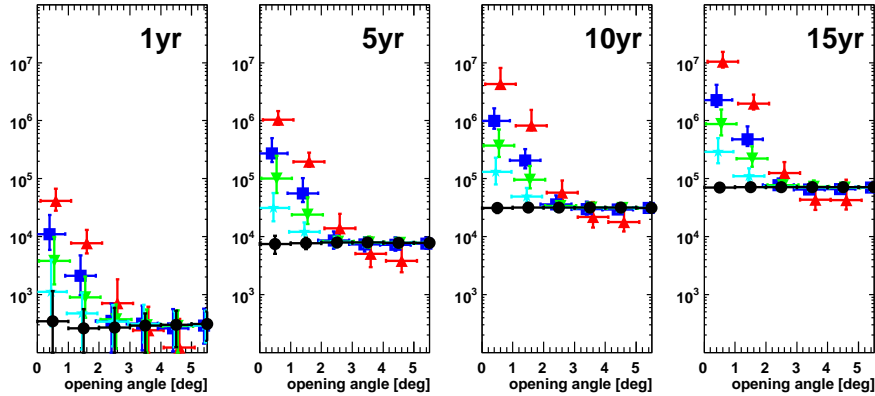


Figure 3. Same as Fig.2 but the minimum distance for nearby sources is $d_{\min}(\bar{\rho})$.

different number densities, we impose a lower limit in the distance to the nearest source and show the constrained angular correlations in Fig. 3. In Fig. 3, the nearest source is at a distance larger than $d_{\min}(\bar{\rho})$, where

$$d_{\min}(\bar{\rho}) = \frac{1}{2} \bar{\rho}^{-1/3} . \quad (6)$$

As can be seen in Fig. 3, imposing a minimum distance alleviates the degeneracies between different source densities after 5 years of full Auger South operations. After the first full year exposure, number densities above 10^{-4} Mpc^{-3} give clear departure from continuous distributions, while for $\lesssim 10^{-3} \text{ Mpc}^{-3}$, 5 years are necessary.

In Table 3, we list the mean number of doublets (\bar{N}_d) expected after 1, 5, 10, and 15 years of Auger South operations for $E > 4 \times 10^{19} \text{ eV}$ and for r between 3 and 6. In the same table we report, along with \bar{N}_d , the asymmetric 1σ errorbars for realizations with a number of doublets above or below the mean. The opening angle used to count doublets is 1° and the realizations have minimum source distance $d_{\min}(\bar{\rho})$ as in Fig. 3. It is worth stressing that \bar{N}_d in the table is the total number of doublets, including doublets inside possible higher multiplicity clusters.

If the number of events used in the simulation is normalized to the low energy spectrum as measured by Auger South, then the number of doublets expected in the future Auger operation are those reported in Table 4.

2.2. Two point correlation function above 10^{20} eV

UHECR clustering and source positions should become easier to identify with events of energies $\gtrsim 10^{20} \text{ eV}$, given that at these energies UHECRs are most likely protons and their trajectories are less likely to be affected by extragalactic and galactic magnetic fields than lower energy events. The difficulty is clearly in the limited statistics of events that can be accumulated in this energy range by Auger South, since the flux is a steeply decreasing power of energy and energy losses that give rise to the GZK feature are also at play in this energy range. A larger array as currently being discussed for the Auger North Observatory should help significantly the ability to do charged particle astronomy at this energy scale.

We simulated the expected angular correlation function in Auger South for events with energies above 10^{20} eV for different source densities. In Fig. 4, the correlation

Table 3. Number of doublets for $E > 4 \times 10^{19}$ eV, using the normalization of the number of simulated events to the number of events observed by Auger above 4×10^{19} eV.

$\bar{\rho}$ (Mpc $^{-3}$)	\bar{N}_d / 1yr	\bar{N}_d / 5yr	\bar{N}_d / 10yr	\bar{N}_d / 15yr
cont.	$0.33^{+0.77}_{-0.33}$	$7.13^{+2.77}_{-2.33}$	$29.7^{+5.3}_{-5.3}$	$67.5^{+8.1}_{-8.3}$
10^{-3}	$1.07^{+2.75}_{-0.80}$	$29.7^{+24.3}_{-12.0}$	125^{+94}_{-49}	279^{+201}_{-104}
10^{-4}	$3.63^{+5.84}_{-2.21}$	$96.7^{+139.1}_{-42.3}$	355^{+318}_{-129}	844^{+647}_{-313}
10^{-5}	$10.6^{+12.0}_{-5.0}$	259^{+217}_{-75}	953^{+619}_{-257}	$2,181^{+1,763}_{-530}$
10^{-6}	$39.6^{+24.6}_{-12.8}$	987^{+408}_{-173}	$4,078^{+3,702}_{-658}$	$9,946^{+4,681}_{-2,010}$

Table 4. Number of doublets for $E > 4 \times 10^{19}$ eV, using the normalization of the number of simulated events to the number of events observed by Auger at low energy.

$\bar{\rho}$ (Mpc $^{-3}$)	\bar{N}_d / 1yr	\bar{N}_d / 5yr	\bar{N}_d / 10yr	\bar{N}_d / 15yr
cont.	$0.92^{+0.99}_{-0.92}$	$22.0^{+4.8}_{-4.6}$	$88.7^{+9.1}_{-9.7}$	200^{+16}_{-12}
10^{-3}	$3.36^{+4.51}_{-2.03}$	$91.0^{+73.0}_{-35.3}$	366^{+300}_{-109}	830^{+562}_{-254}
10^{-4}	$11.0^{+19.6}_{-5.6}$	269^{+338}_{-101}	$1,031^{+821}_{-373}$	$2,448^{+1,754}_{-874}$
10^{-5}	$31.3^{+35.1}_{-12.6}$	773^{+664}_{-222}	$2,814^{+1,831}_{-757}$	$6,457^{+5,427}_{-1,540}$
10^{-6}	114^{+46}_{-27}	$2,884^{+1,315}_{-419}$	$11,914^{+10,889}_{-1,815}$	$29,369^{+13,356}_{-5,831}$

function is shown for sources located at minimum distances $d_{\min}(\bar{\rho})$ as in Fig. 3. In addition, we fixed the number of events above 10^{20} eV to the mean number given in Table 1. If we let the number of events fluctuate between realizations, the error bars are significantly enhanced. In principle, once Auger has run for 5 years, we will know the number of events above 10^{20} eV. As discussed below, the number of events expected above 10^{20} eV for a fixed injection spectrum, depends on the source density. Combining a study of the GZK feature with the small scale anisotropies should yield $\bar{\rho}$. As shown in Fig. 3, a departure from a continuous source distribution is detectable at the 1σ level after 5 years for $\bar{\rho} \lesssim 10^{-5}$ Mpc $^{-3}$. Larger densities require 10 to 15 years before clear detectability. Even after a decade, distinguishing between different source densities will be a major challenge.

In Table 5 we show the predicted number of doublets at energies above 10^{20} eV

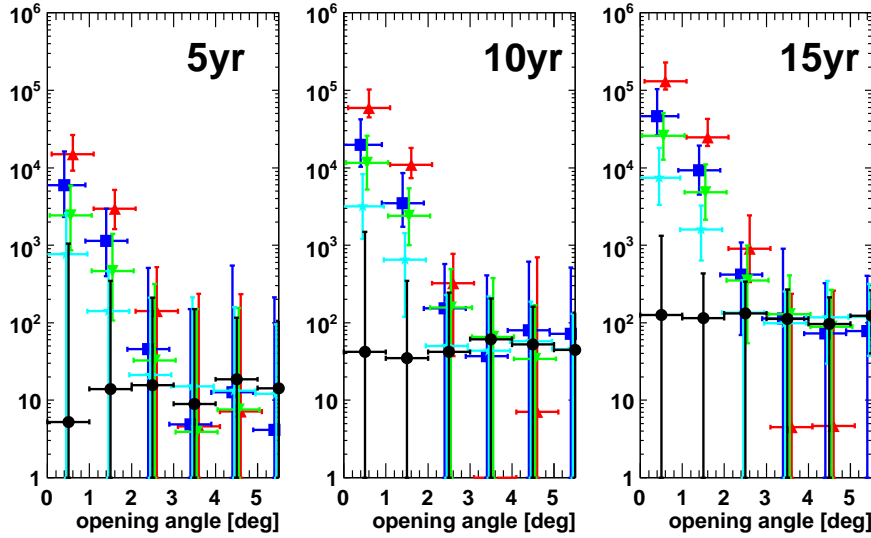


Figure 4. Two point correlation function for events above 10^{20} eV after 5, 10, and 15 years at Auger South for a continuous distribution of sources (black circles), and number densities of 10^{-3} Mpc^{-3} (cyan stars), 10^{-4} Mpc^{-3} (green downward triangles), 10^{-5} Mpc^{-3} (blue squares), and 10^{-6} Mpc^{-3} (red upward triangles). The minimum distance for the nearest source is $d_{\min}(\bar{\rho})$.

Table 5. Number of doublets for $E > 10^{20}$ eV with normalization to the Auger data above 4×10^{19} eV.

$\bar{\rho}$ (Mpc^{-3})	$\bar{N}_d / 5\text{yr}$	$\bar{N}_d / 10\text{yr}$	$\bar{N}_d / 15\text{yr}$
cont.	$0.02^{+1.40}_{-0.02}$	$0.04^{+1.38}_{-0.04}$	$0.12^{+1.15}_{-0.12}$
10^{-3}	$0.73^{+1.76}_{-0.73}$	$3.05^{+4.84}_{-1.90}$	$7.09^{+10.11}_{-3.91}$
10^{-4}	$2.32^{+3.28}_{-1.50}$	$11.1^{+13.7}_{-6.1}$	$24.8^{+23.9}_{-12.6}$
10^{-5}	$5.71^{+9.77}_{-3.48}$	$19.0^{+21.6}_{-9.1}$	$44.4^{+54.6}_{-19.4}$
10^{-6}	$14.3^{+11.0}_{-5.6}$	$56.8^{+41.6}_{-14.2}$	125^{+94}_{-27}

after 5, 10, and 15 years of operation of Auger south for different values of the source density.

As stressed in the previous section, the number of events at energies above 10^{20} eV is estimated by using as a normalization the flux currently observed by Auger South at 4×10^{19} eV. However, as shown in Fig. 1, the observed spectrum appears to be at odds with the observed low energy spectrum. If the solid line in Fig. 1 is used for the normalization of the number of events above 10^{20} eV, then the situation

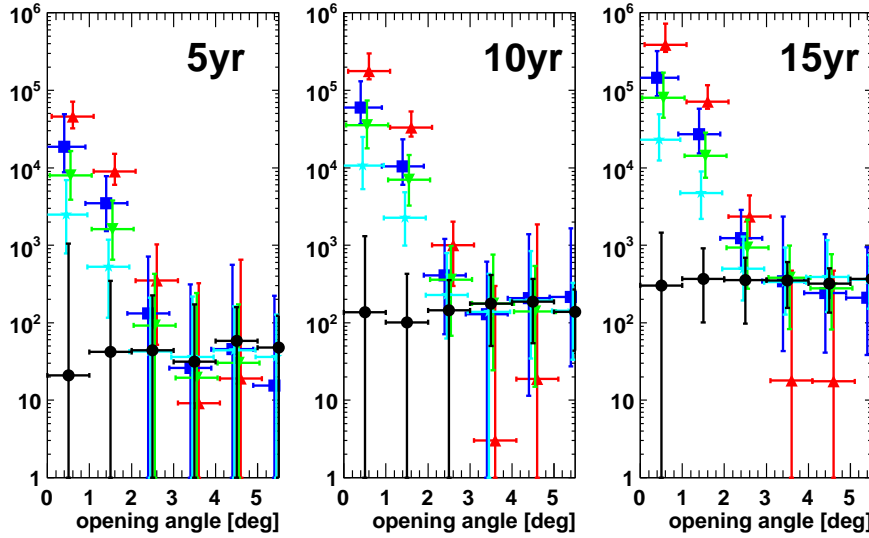


Figure 5. Two point correlation function for events above 10^{20} eV after 5, 10, and 15 years at Auger South for a continuous distribution of sources (black circles), and number densities of 10^{-3} Mpc^{-3} (cyan stars), 10^{-4} Mpc^{-3} (green downward triangles), 10^{-5} Mpc^{-3} (blue squares), and 10^{-6} Mpc^{-3} (red upward triangles). The minimum distance for the nearest source is $d_{\min}(\bar{\rho})$.

Table 6. Number of doublets for $E > 10^{20}$ eV with normalization to the low energy Auger data.

$\bar{\rho}$ (Mpc^{-3})	$\bar{N}_d / 5\text{yr}$	$\bar{N}_d / 10\text{yr}$	$\bar{N}_d / 15\text{yr}$
cont.	$0.02^{+0.98}_{-0.02}$	$0.19^{+0.98}_{-0.19}$	$0.39^{+1.05}_{-0.39}$
10^{-3}	$3.29^{+5.08}_{-2.08}$	$13.9^{+15.4}_{-7.1}$	$30.0^{+32.6}_{-13.8}$
10^{-4}	$10.5^{+9.5}_{-5.3}$	$46.8^{+50.1}_{-22.8}$	102^{+104}_{-46}
10^{-5}	$23.9^{+33.4}_{-12.5}$	$76.8^{+94.3}_{-29.4}$	187^{+220}_{-78}
10^{-6}	$59.6^{+33.9}_{-17.9}$	228^{+168}_{-46}	503^{+413}_{-93}

improves somewhat (the number of events above 10^{20} eV is roughly doubled in this case). This is shown in Fig. 5, where we plot the two point correlation function for the new number of events above 10^{20} eV after 5, 10, and 15 years.

The number of doublets obtained for this second instance of normalization to the data is shown in Table 6.

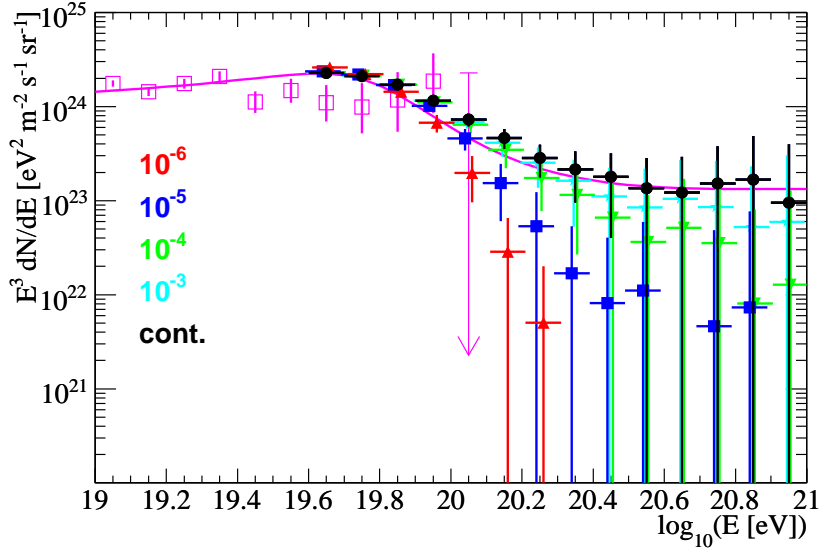


Figure 6. Energy spectrum for different source densities compared with Auger data (open squares). The sources densities are 10^{-6} Mpc^{-3} (red upward triangles); 10^{-5} Mpc^{-3} (blue squares), 10^{-4} Mpc^{-3} (green downward triangles); 10^{-3} Mpc^{-3} (cyan stars); and a continuous distribution of sources (black circles).

2.3. Spectra for different number densities

As shown in [13] the combination of small angle clustering and spectral informations is a powerful tool to investigate the nature of the sources of UHECRs. A low density of sources would in fact be responsible for more evident small angle clustering of the arrival directions, but at the same time would also induce a sharper shape of the GZK feature, and therefore a lower number of events at the highest energies. A larger density of sources has the opposite effect: the GZK feature is shallower (more events at the highest energies) but the clustering is mild. As pointed out in [13], the AGASA data on the small scale anisotropies appear to be at odds with the spectrum, as measured by the same experiment.

Here we investigate the potential to use a similar technique for the data of the Pierre Auger Observatory.

In Fig. 6, we show the energy spectrum around the GZK feature that may be detected by Auger South after 15 years of full aperture operations, assuming the normalization at low energy. The spectrum is shown for different source densities ranging from a continuous source distribution (black circles) to source densities between 10^{-3} Mpc^{-3} (cyan stars) and 10^{-6} Mpc^{-3} (red upward triangles). Also shown is the first release of the Auger spectrum (open magenta squares) [24] and an analytical prediction (continuous line).

The number of events at energy above 10^{20} eV is a rather sensitive function of the source density, as can also be understood from Tables 1 and 2. For the case of normalization at low energy, one could have as many as ~ 75 events above 10^{20} eV in 15 years of operation of Auger South, for a continuous (and unlikely) distribution

of sources, or as little as ~ 13 events in the same energy region if the sources have a mean local density 10^{-6}Mpc^{-3} . Unfortunately this also means that the statistical uncertainties in the fluxes at the highest energies become large if the source density is too low, and it becomes correspondingly harder to have a precision measurement of the shape of the GZK feature in these cases. For source densities between 10^{-6}Mpc^{-3} and 10^{-5}Mpc^{-3} Auger is expected to become statistics dominated at energies $\sim 10^{20.2}$ eV. However at this energy the different predicted spectra already differ from that generated by a continuous source distribution by about a factor ~ 10 . Again, the combination of spectra measurements and anisotropy measurements can play an instrumental role in inferring hints to the nature of the sources of UHECRs.

3. Conclusions

The imminent completion of the Auger Observatory in Argentina will mark the beginning of a new era in cosmic ray astrophysics. The combination of a very large ground array and fluorescence telescopes will provide a detailed measurement of the spectrum at the highest energies.

One of the main open questions in Cosmic Ray Physics is the presence of a GZK feature in the spectrum. If this feature is in fact there, it becomes very important to measure its shape, which can provide us with information on the number of sources and their spatial distribution. Independently of the presence or absence of the GZK feature, the problem of finding an acceleration mechanism and a class of sources that may harbor the accelerator remains of paramount importance. Auger will most likely clarify whether the spectrum of UHECRs has or not the GZK suppression. In order to answer the second big question, we need high quality information (namely high statistics) about the directions of arrival of UHECRs, and their chemical composition. The first hints of such new era of charged particle astronomy are likely to come from small deviations from isotropic distributions in the next few years of Auger South operations.

In this paper we made quantitative predictions of the amount of small scale anisotropies expected in Auger in the next decade for a range of plausible source densities. We investigated two instances of normalization of the number of events expected at the highest energies, depending on whether the procedure is applied to the data measured by Auger at 4×10^{19} eV or rather at lower energies where statistical errors should be less important. The amount of small angle clustering has been quantified through the two point correlation function, both for events above 4×10^{19} eV and above 10^{20} eV. We conclude that it will be sufficient to run Auger for a few years to detect the departure of the two point correlation function from that expected from a continuous distribution of sources. On the other hand, it will be more problematic to measure the mean source density with high accuracy, because of the relatively low number of events and correspondingly large statistical fluctuations. As already proposed in [13], the combination of small angle clustering and spectrum of diffuse cosmic rays is able to provide us with more stringent constraints on the source density. This will be true for Auger as well, although the statistical error bars on the spectrum for the case of discrete sources, as shown in Fig. 6, are expected to become relatively large at energies around $10^{20.2}$ eV. This result is rather more pessimistic than the ones previously obtained in [21] because such previous results were obtained adopting the normalization (not the shape) of the AGASA spectrum, which has now been found to lead to cosmic ray fluxes about three times larger than those actually

measured by Auger at the present time.

Despite these problems, it is fair to conclude that once the departures from isotropy will be detected, the estimate of the mean density of sources, $\bar{\rho}$ will be within reach. The even more challenging possibility of measuring the spectrum of a single source [12] will require a significant increase in statistics at the highest energies as currently being discussed in the context of the Auger North Observatory or future generation cosmic ray observatories, that will most likely be located in space.

Acknowledgments

The work of D.D.M. is funded through NASA APT grant ATP03-0000-0080 at University of Delaware. The research of P.B. is funded through COFIN2004/2005. This work was supported in part by the KICP under NSF PHY-0114422 and by NSF PHY-0457069, at the University of Chicago.

References

- [1] Greisen K 1966 *Phys. Rev. Lett.* **16** 748
Zatsepin G T and Kuzmin V A 1966 *Sov. Phys. JETP Lett.* **4** 78
- [2] Cronin J W 2001 *Pierre Auger Observatory, Proceedings of ICRC 2001*
Cronin J W 2005 *Nuclear Physics B (Proc. Suppl.)* **138** 465
- [3] Sommers P 2001 *Astropart. Phys.* **14** 271
- [4] Dolag K, Grasso D, Springel V and Tkachev I 2005 *J. Cosmol. Astropart. Phys.* JCAP01(2005)009
Dolag K, Grasso D, Springel V and Tkachev I 2004 *JETP Lett.* **79** 583
Dolag K, Grasso D, Springel V and Tkachev I 2004 *Pisma Zh. Eksp. Teor. Fiz.* **79** 719
- [5] Allard D, Parizot E, Khan E, Goriely S and Olinto A V 2005 *Preprint astro-ph/0505566*
- [6] Allard D, Parizot E, and Olinto A V 2005 *Preprint astro-ph/0512345*
- [7] Berezhinsky V, Gazizov A Z and Grigorieva S I 2002 *Preprint hep-ph/0204357*
Berezhinsky V, Gazizov A Z and Grigorieva S I 2002 *Preprint astro-ph/0210095*
Berezhinsky V, Gazizov A Z and Grigorieva S I 2002 *Proc. of Int. Workshop "Extremely High-Energy Cosmic Rays" (eds M. Teshima and T. Ebisuzaki), Universal Press, Tokyo, Japan, p. 63*
Berezhinsky V, Gazizov A Z and Grigorieva S I 2005 *Phys. Lett.* **B612** 147
- [8] Sigl G and Armengaud E 2005 *J. Cosmol. Astropart. Phys.* JCAP10(2005)016
- [9] Kachelriess M and Semikoz D 2005 *Preprint astro-ph/0510188*
- [10] Sigl G, Miniati F and Ensslin T 2004 *Phys. Rev.* **D70** 043007
- [11] Armengaud E, Sigl G and Miniati F 2005 *Phys. Rev.* **D72** 043009
- [12] Blasi P and De Marco D 2004 *Astropart. Phys.* **20** 559
- [13] De Marco D, Blasi P and Olinto A V 2006 *J. Cosmol. Astropart. Phys.* JCAP01(2006)002
- [14] Blasi P, Burles S and Olinto A V 1999 *Astrophys. J. Lett.* **514** L79
- [15] Lemoine M 2005 *Phys. Rev.* **D71** 083007
- [16] Deligny O, Letessier-Selvon A and Parizot E 2004 *Astropart. Phys.* **21** 609
- [17] Takeda M *et al* 1999 *Astrophys. J.* **522** 225
Uchihori Y *et al* 2000 *Astropart. Phys.* **13** 151
Hayashida N *et al* 2000 *Preprint astro-ph/0008102*
- [18] Finley C B and Westerhoff S 2004 *Astropart. Phys.* **21** 359
- [19] Isola C and Sigl G 2002 *Phys. Rev.* **D66** 3002
- [20] Yoshiguchi H, Nagataki S, Tsubaki S and Sato K 2003 *Astrophys. J.* **586** 1211
Yoshiguchi H, Nagataki S and Sato K 2003 *Astrophys. J.* **592** 311
Takami H, Yoshiguchi H, Sato K 2005 *Preprint astro-ph/0506203*
Dubovsky S L, Tinyakov P G and Tkachev I I 2000 *Phys. Rev. Lett.* **85** 1154
Fodor Z and Katz S D 2001 *Phys. Rev.* **D63** 023002
- [21] De Marco D, Blasi P and Olinto A V 2003 *Astropart. Phys.* **20** 53
- [22] Berezhinsky V and Grigorieva S 1988 *Astron. Astroph.* **199** 1
- [23] Yoshiguchi H, Nagataki S and Sato K 2003 *Preprint astro-ph/0302508*

- [24] Sommers P *et al* (Auger Collaboration) 2005 *Proceedings of ICRC 2005, Pune, India, Preprint* astro-ph/0507150
- [25] Takeda M *et al* 1998 *Phys. Rev. Lett.* **81** 1163
Hayashida N *et al* 2000 *Astron.J.* **120** 2190
- [26] Berlind A A *et al* (SDSS Collaboration) 2006 *Preprint* astro-ph/0601346